substance: boron compounds with lanthanides
property: properties of lanthanide hexaborides: YbB_6

Structure, chemical bond

Structure: cubic

Space group: Pm3m

Single crystal preparation by the aluminium-flux method [94O].

X-ray diffraction (compared with LaB_6, CaB_6 and ThB_6) [82B].

Growth and crystal data for preparation by high temperature solution growth [84L] and references therein.

lattice parameters

a	4.1479(1) Å		single crystal, X-ray diffraction	95B
	4.1474(5) Å	*T* = 300 K		94O
V	71.34(4) $Å^3$			
a	4.1478 Å	*T* = 300 K	seealso [56P]	70E2, 77E, 79G

interatomic distances
(in Å)

d	1.7525(12)	B – B	95B
	1.6695(17)	B – B’	
	3.0495(3)	B – Me	

Electronic properties

energy gaps (or activation energies for conduction)

E_g	0.14 eV	electrical conductivity		77E, 73G
	0.081 eV			80L

pressure dependence of the energy gap

dE_g/dp	– 3.7meV/kbar	*T* = 300 K	80L

optical transition energies
(in meV):

E_g	7.45(5)	*T* = 300 K	impurity to band	99W
	10.4(2)		impurity to band or direct forbidden interband	
	15.2(5)		direct allowed interband	
	26.0(4)		direct allowed interband	
δE_C	11	*T* = 300 K	carbon donor level (estimated from carrier concentration depending on C content)	99W

FIR absorption spectrum in Fig. 1 [99W].

effective mass of electrons

m_n	0.47 m_0	*T* = 300 K	estimated from plasma frequency in analogy to EuB_6	99W

Impurities and defects

lattice parameters

a	4.1476(5) Å	*T* = 300 K	X-ray diffraction, nominal compound $YbB_{5.97}C_{0.03}$	81T

ESR study of $EuB_{6-x}C_x$ including the comparison with some corresponding $YbB_{6-x}C_x$, $SrB_{6-x}C_x$, $Eu_{1-x}Gd_xB_6$, $Eu_{1-x}Sr_xB_6$ and $Eu_{1-x}La_xB_6$ compounds in [81T].

For the relation between carrier concentration and carbon content compared with EuB_6 see Fig. 2 [81T, 99S, 99W].

Lattice properties

For vibrational frequencies [88T, 90Y, 93Y]

Thermal expansion coefficient: α [$10^{-6}K^{-1}$] = 4.1477 (1+5.78 10^{-6} T + 1.70 10^{-9} T^2), T in K [73D].

For force constants [90Y]

Theoretical study of the lattice dynamics; calculated phonon dispersion curves in Fig. 3 [85T].

IR phonon wavenumbers

v/*c*	873.6 cm^{-1}	*T* = 300 K		99W
	110.2 cm^{-1}			

elastic constants

(in 10^{11} dyn cm^{-2})

c_{11}	33.69	calculated (one specific model)	85T
	33.5	experimental	
c_{12}	8.11	calculated	85S
	8.1	experimental	
c_{44}	4.07	calculated	
	4.0	experimental	
	4.1	experimental	
c_{bulk}	16.6		

Transport properties

conductivity

σ	40 Ω^{-1} cm^{-1}	*T* = 300 K	see Fig. 4	73G, 77E
	30 Ω^{-1} cm^{-1}			73M

resistivity

ρ	$0.52 \cdot 10^{-3}$ Ω cm	*T* = 300 K		94O
	$0.466 \cdot 10^{-4}$ Ω cm			80S

Pressure dependence of the electrical resistivity; $\rho(p)/\rho(0)$ vs. hydrostatic pressure p (compared with LaB_6, SmB_6 and EuB_6) in Fig. 5 [81K, 91S].

temperature coefficient of resistivity

$(1/\rho)d\rho/dT$	$+ 0.234 \cdot 10^{-2}$ K^{-1}	*T* = 300 K	75S

pressure dependence of resistivity

$(\mathrm{d} \log \rho/\mathrm{d}p)_{p=0}$	$-65 \cdot 10^{-3}$ kbar^{-1}	T = 300 K		80L

thermoelectric power

S	– 190 μV K^{-1}	T = 300 K	see Fig. 6; see also [73M]	73G
	– 25.5 μV K^{-1}			75S
	+ 18.4 μV K^{-1}			69P
	– 185 μV K^{-1}	T = 300 K		91S

Pressure dependence of the thermoelectric power in Fig. 7 [81K, 91S].

For Hall coefficient, see [62S].

For electrical properties of YbB_6, see also [70P, 81K].

Optical properties

Raman spectra of SmB_6 and LaB_6 are shown in Fig. 8. For Raman frequencies of SmB_6, EuB_6, YbB_6, see Fig. 9. The reflectivity and dielectric function of SmB_6 is shown in Fig. 10. The reflectivity of EuB_6 and LaB_6 is given in Fig. 11. A Raman spectrum of EuB_6 is presented in Fig. 12.

lattice dielectric constant
(derived by extrapolating ε_r in the range of the plasma edge, see Fig. 1)

ε_L	7.0(2)	T = 300 K	single crystal, high-purity (C< 0.1 at. %)	99W

IR diffuse reflection and Raman spectra (La, Nd, Gd, Tb, Dy, Yb)B_6 in Fig. 13 [88T, 93Y].
IR reflectivity spectrum in Fig. 14 [99W].

Further properties

density

d	5.484 g cm^{-3}	T = 300 K	pycnometric	94O
	5.538(2) g cm^{-3}		X-ray	
	5.556 g cm^{-3}		X-ray	75S
	5.53 g cm^{-3}		X-ray	69M2
	4.37 g cm^{-3}		pycnometric	75S
	5.45 g cm^{-3}		pycnometric	69M2

microhardness

H_V	22.1(15) GPa	T = 300 K		94O
	26.6 GPa			80S
H_K	2140 kg mm^{-2}	T = 300 K	cube, average value; load 50 g,	96G
	1910 kg mm^{-2}		cube, average value; load 200 g	
	1850 kg mm^{-2}		rhombododecahedron, average value; load 50 g	
H	3080 kg mm^{-2}	T = 300 K	hardness not specified	75S

Debye temperature

Θ_D	265 K		lattice dynamics	85S

Specific heat depending on T in Fig. 15 [85S].

melting point

T_m	> 2500°C			80H

linear thermal expansion coefficient

α	$5.85 \cdot 10^{-6}$ K^{-1}	T = 300 K		75S

work function

Φ	3.13 eV		75S
emissivity at 655 mn			
ε	0.7		75S
magnetic moment			
p_{eff}	4.58 μ_{B}	effective magnetic moment	67P
magnetic susceptibility			
χ_{m}	$8740 \cdot 10^{-6}$ cm^3 mol^{-1} T = 300 K	χ_{m} in CGS-emu	75S
asymptotic (paramagnetic) Curie temperature			
Θ_{a}	– 161 K		77B2

References:

56P Post, B., Moskowitz, D., Glaser, F. W.: J. Am. Chem. Soc. 78 (1956) 1800.

62S Samsonov, G. V., Vainshtein, E. Y., Paderno, Y. B.: Fiz. Metal. Metallov. 13 (1962) 764

67P Paderno, Yu. B., Pokrzywnicki, S., Stalinski, B.: Phys. Status Solidi 24 (1967) K 73.

69F Fisk, Z.: Ph. D. Thesis, Univ. California, 1969.

69M1 Menth, H., Buehler, E., Geballe, T. H.: Phys. Rev. Lett. 22 (1969) 295.

69M2 Mercuno, J. P.: C. R. Acad. Sci. colon 268 (1969) 1766.

69P Paderno, Yu. B., et al.: Poroshk. Metall. Acad. NAUK Ukr. SSR 10 (1969) 55.

70E1 Boron 3, T. Niemyski, ed., PWN Warsaw, 1970

70E2 Etourneau, J., Mercuno, J. P., Naslain, R., Hagenmuller, P.: J. Solid State Chem. 2 (1970) 332.

70P Paderno, Yu. B., Goryachev, Yu. M., Garf, E. S.: see [70E1] p. 175.

71N Nickerson, J. C., White, R. M., Lee, K. N., Bachmann, R., Geballe, T. H., Hull, G. W. Jr.: Phys. Rev. B 3 (1971) 2030.

73B Budozhapov, V. D., Zelenin, L. P., Chemerinskaya, L. S., Sidorenko, F. A., Gel'd, P. V.: Izv. Akad. NAUK SSSR Neorg. Mater. 9 (1973) 1447.

73D Dudchak, Ya.I., Fedishin, Ya.I., Paderno, Yu.B., Vadez, D.I.: Izv. Akad. Nauk. SSSR Ser. Fiz. 1 (1973) 154 (in Russian).

73G Goodenough, J. B., Mercurlo, J. P., Etourneau, I., Naslain, R., Hagenmuller, P.: C. R. Acad. Sci. (Paris) 277 (1973) 1239.

73M Mercurio, J. P., Etourneau, J., Naslain, R., Hagenmuller, P.: Mater. Res. Bull. 8 (1973) 837.

75S Samsonov, G. V., Serebryakova, T. I., Neronov, V. A.: Boridy, Moskva Atomizdat, 1975.

76I Ishii, M., Aono, M., Muranaka, S., Kawai, S.: Solid State Commun. 20 (1976) 437.

77B1 Berezin, A. A., Golikova, O. A., Zaitsev, V. R., Kazanin, M. M., Orlov, V. M., Tkalenko, E. N., in:Boron and Refractory Borides, (Matkovich V. 1., ed.) Springer: Berlin, Heidelberg, New York 1977, p. 52.

77B2 Busehow, K. H. J.: see [77B1], p. 494.

77E Etourneau, J., Mercuno, J. P., Hagenmuler, P.: see [77B1], p. 115.

77K Kasuya, T., Kojima, K., Kasaya, M.: see [77A], p. 137.

78A Allen, J. W., Martin, R. M., Batlogg, B., Wachter, P.: J. Appl. Phys. 49 (1978) 2078.

79F Fisk, Z., Johnston, D. C., Cornut, B., v. Molnar. S., Oserov, S. . Calvo, R.: J. Appl. Phys. 50 (1979) 1911.

79G Gurin, V. N., Korsukova, M. M., Nikanorov, S. P., Smirnov, I. A., Stepanov, N. N., Shulman, S. G.: J. Less-Common Met. 67 (1979) 115.

80G Gurin, V. N., Korsukova, M. M., Karin, M. G., Sidorin, K. K., Smirnov, I. A., Shelikh, A. I.: Sov. Phys. Solid. State 22 (1980) 418.

80H Holtzberg, F., v. Molnar, S., Coly, J. M. D.: Handbook on Semicond., Vol. 3 (ed. Keller, S. P.) North Holland: Amsterdam, 1980, p. 803.

80L Lannin, J.S., Messier, R.: Phys. Rev. Lett. 45 (1980) 1119.

80S Samsonov, G.V., Vinitskii, I.M.: in: Handbook of Refractory Compounds, IFI/Plenum: New York, 1980, p. 143.

81A Armstrong, D. R.: Proc. 7th Int. Symp. Boron, Borides and Related Compounds. Uppsala, Sweden, 1981; spec. issue of J. Less-Common Met. 82 (1981) 357.

81K Korsukova, M.M., Stepanov, N.N., Gontcharova, E.V., Gurin, V.N., Nikanorov, S.P., Smirnov, I.A.: J. Less-Common Met. 82 (1981) 211. (Proc. 7th Int. Symp. Boron, Borides and Rel. Compounds, Uppsala, Sweden, 1981).

81M Mörke, I., Dvorak, V., Wachter, P.: Solid State Commun. 40 (1981) 331.

81S Shelich, A. I., Sidorin, K. K., Karin, M. G., Bobrikov, V. N., Korsukova, M. M., Gurin, V. N., Smirnov, I. A., (abstract only): see [81A1], p. 291.

81T Tarascon, J.M., Etourneau, J., Dance, J.M., Hagenmuller, P., Georges, R., Angelov, S., v. Molnar, S.: J. Less-Common Met. 82 (1981) 277 (Proc. 7th Int. Symp. Boron, Borides and Rel. Compounds, Uppsala, Sweden, 1981).

81W Werheit, H., de Groot, K., Malkemper, W.: see [81A1], p. 153.

82B Barantseva, I.G., Paderno, Yu.B.: Sov. Powder Metall. Met. Ceram. 21 (1982) 585.

84L Lundström, T.: J. Less-Common Met. 100 (1984) 215.

85S Smith, H.G., Dolling, G., Kunii, S., Kasaya, M., Liu, B., Takegahara, K., Kasuya, T., Goto, T.: Solid State Commun. 53 (1985) 15.

85T Takegahara, K., Kasuya, : Solid State Commun. 53 (1985) 21.

88T Turrell, S., Yahia, Z., Huvenne, J.P., Lacroix, B., Turrell, G.: J. Mol. Struct. 174 (1988) 455.

90Y Yahia, Z., Turrell, S., Turrell, G., Mercurio, J.P.: J. Mol. Struct. 224 (1990) 303.

91S Sidorov, V.A., Stepanov, N.N., Ziok, O.B., Chvostanzev, L.G., Smirnov, N.A., Korsukova, M.M.: Fiz. Tverd. Tela 33 (1991) 1271(in Russian).
93Y Yahia, Z., Turrel, S., Mercurio, J.P., Turrel, G.: J. Raman Spectroscopy 24 (1993) 207.
94O Okada, S., Kudou, K., Yu, Y., Lundström, T.: Proc. 11th Int. Symp. Boron, Borides and Rel. Compounds, Tsukuba, Japan, August 22 - 26, 1993, Jpn. J. Appl. Phys. Series 10 (1994), p. 136.
95B Blomberg, M.K., Merisalo, M.J., Korsukova, M.M., Gurin, V.N.: J. Alloys Compounds 217 (1995) 123.
96G Gurin, V.N., Derkachenko, L.I., Korsukova, M.M., Nikanorov, S.P., Jung, W., Müller, R.: Sov. Phys. Solid State 38 (1996) 1508.
99S Schwetz, K.: (personal communication).
99W Werheit, H., Au, T., Schmechel, R., Paderno, Yu.B., Konovalova, E.S.: J. Solid State Chem. (2000) (Proc. 13th Int. Symp. Boron, Borides and Rel. Compounds, Dinard, France, Sept. 1999).

Fig. 1.

YbB_6. FIR absorption spectrum calculated from the reflectivity spectrum using a Kramers-Kronig transformation. Empirical slope for the free carrier absorption ($\propto \lambda^2$ for phonon scattering) subtracted from the measured absorption approximately yields the interband absorption (lower curve).[99W].

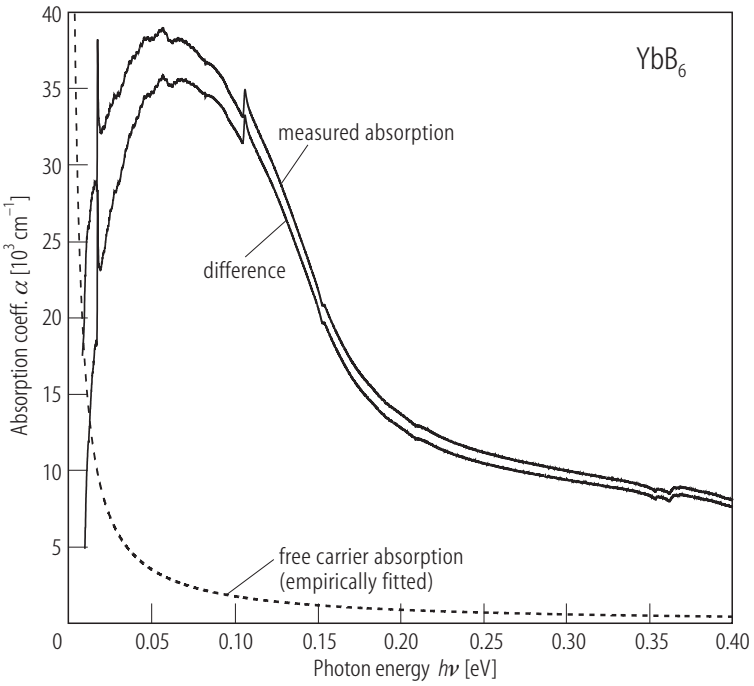

Fig. 2.

EuB_6:C, YbB_6:C. EuB_6: Carrier concentration vs. C content; data at C =0.43 at. % and 0.71 at. % from [81T]. The points for the pure crystals suggest that the upper limit of 0.1 at.% C, given for the purest samples, is too high and the real C content is about 0.05 at. % only. The arrow marks the relation between the chemically determined total C content of 1.1 at.% and that one in the EuB_6 lattice, which according to experience is roughly estimated to be about 25 % lower in sintered EuB_6 [99S]. YbB_6: Only the data for 0.43 at. % C [81T] and upper carbon limit for the pure crystal are available. A dependence similar to that of EuB_6 is assumed [99W].

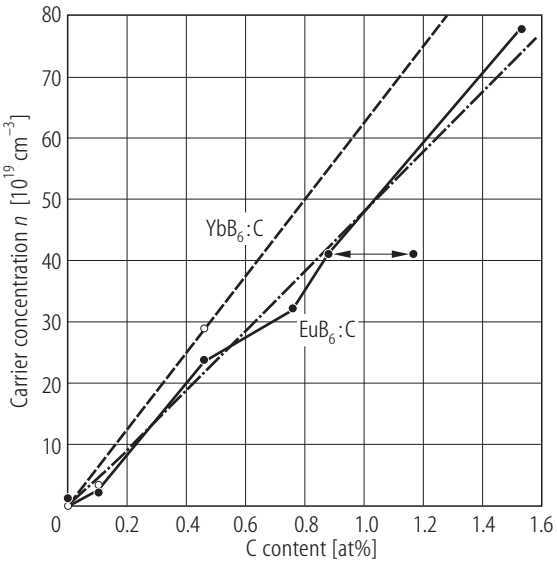

Fig. 3.

YbB_6. Calculated phonon dispersion curves. The dashed lines have been calculated from the observed sound velocities. Frequencies measured by Raman are shown by open circles [85T].

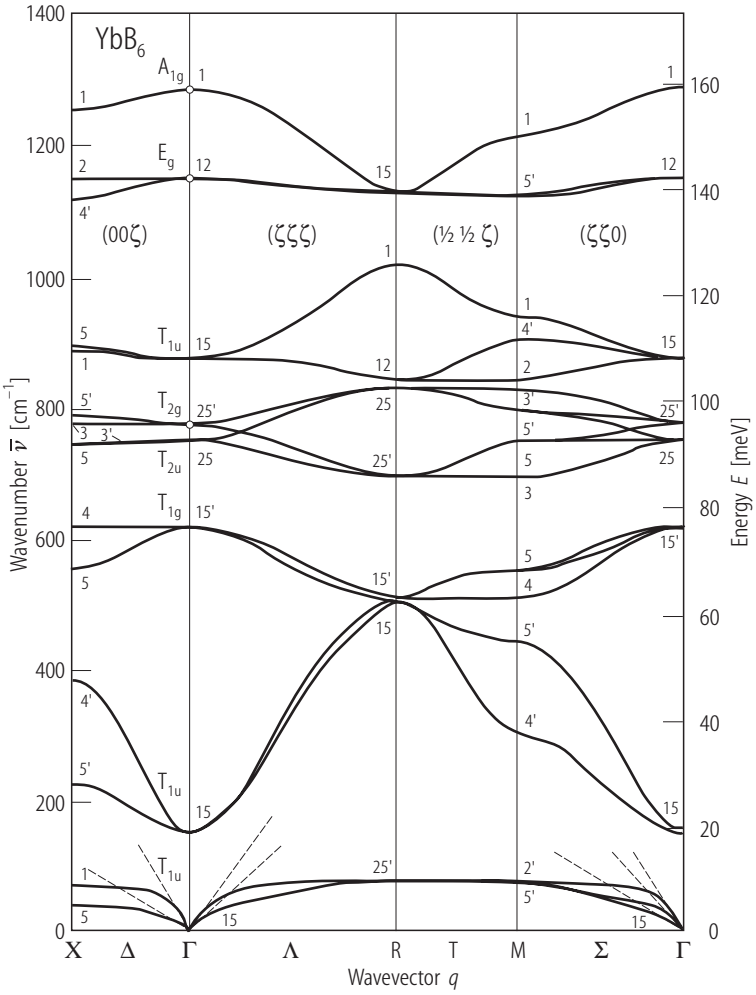

Fig. 4.

EuB_6, YbB_6. Electrical conductivity vs. reciprocal temperature [77E, 73M, 73B]. Cp. also [69F, 75S].

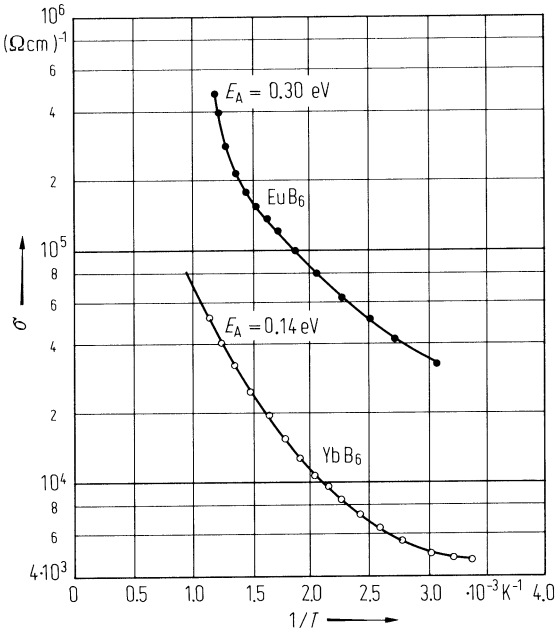

Fig. 5.

Metal hexaborides. Pressure dependence of the electrical resistivity; $\rho(p)/\rho(0)$ vs. hydrostatic pressure p. Full lines, monocrystalline LaB_6, EuB_6 and YbB_6 [91S10], dashed lines, LaB_6, SmB_6 prepared from starting ratios Sm:B 1/7, 1/9, 1/12 (effect increases this way), YbB_6, EuB_6 [81K].

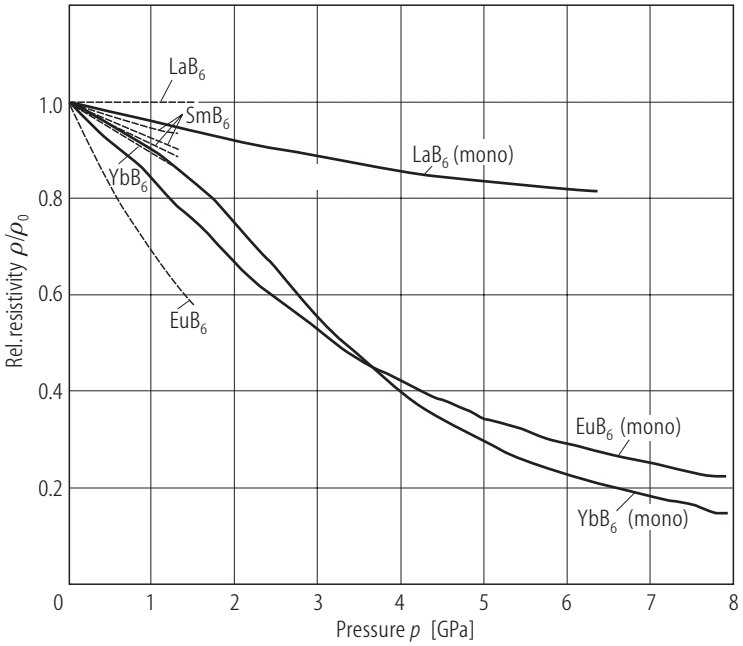

Fig. 6.

EuB_6, YbB_6. Thermoelectric power vs. temperature [77E, 73M, 73B]. Cp. also [75S].

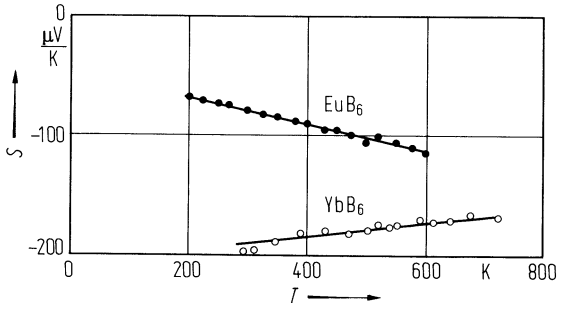

Fig. 7.

Metal hexaborides. Pressure dependence of the thermoelectric power S for LaB_6, YbB_6 and EuB_6 [81K].

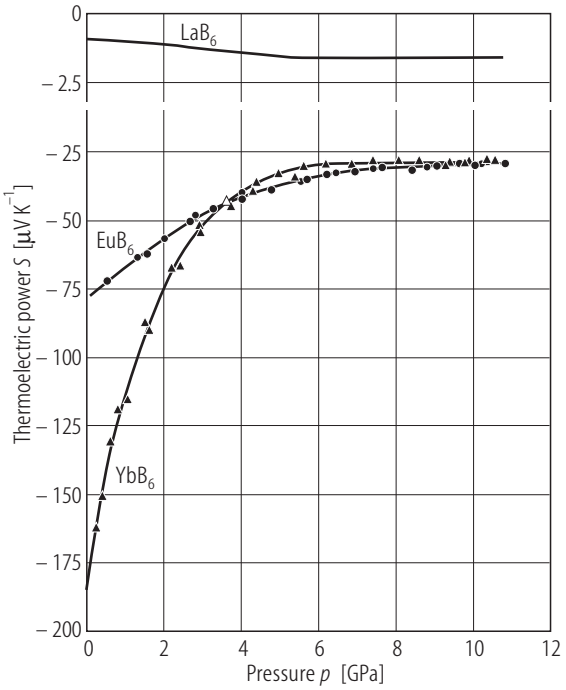

Fig. 8.

LaB_6, SmB_6. Room temperature Raman spectra of single crystals. Experimental conditions: oblique back scattering, laser 50 mW, λ = 514 nm, resolution 8 cm^{-1} [81M].

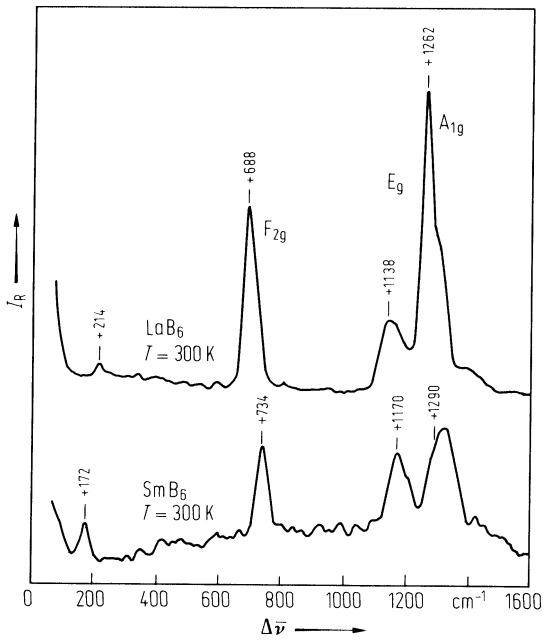

Fig. 9.

SmB_6, EuB_6, YbB_6 (and other MB_6). Raman wavenumbers of metal hexaborides with bivalent and trivalent metals vs. lattice constant [76I].

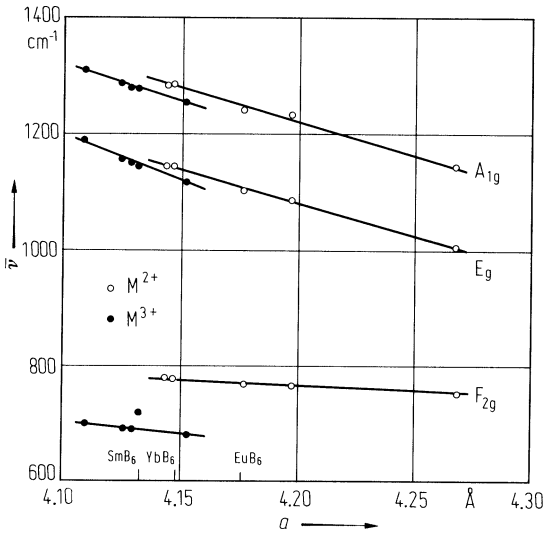

Fig. 10.

SmB_6. Reflectivity and dielectric functions (calculated by Kramers-Kronig analysis) vs. phonon energy [77A, 78A]. The dielectric functions which are calculated according to two different extrapolations (*1*) (*2*) of the experimental reflectivity towards low photon energies, show that there are two limiting types of behavior, which cannot be distinguished at present because of the experimental uncertainty. Zero crossings of a are indicated by arrows.

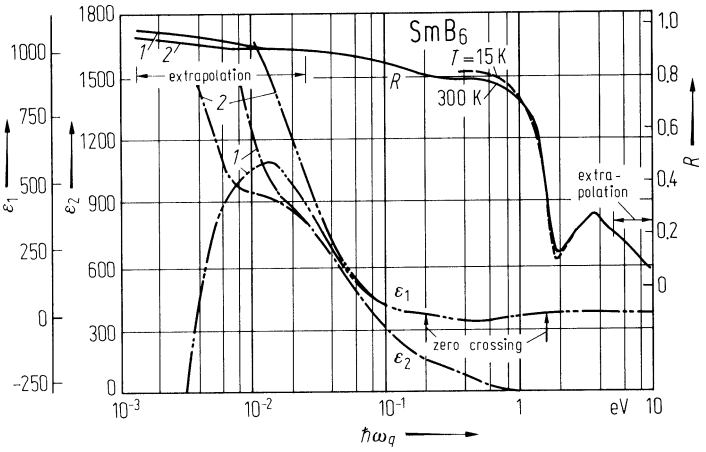

Fig. 11.

EuB_6, LaB_6. Reflectivity vs. photon energy [80G]. For permittivity spectra derived from the reflectivity, see [80G].

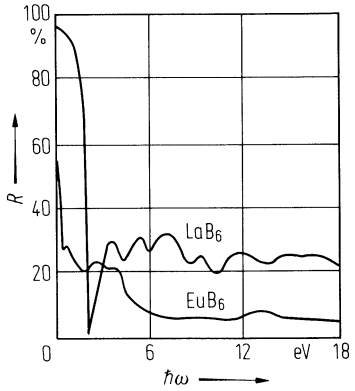

Fig. 12.

EuB_6. Raman spectrum. Scattering intensity vs. wavenumber (488 nm excitation) [76I].

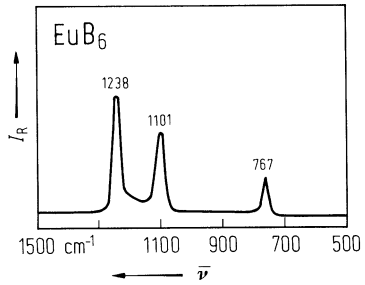

Fig. 13.

Metal hexaborides. IR diffuse reflectance spectra of representative MB_6 compounds with two-valent Ca, Sr and Yb, and three-valent Nd, Gd, La, Tb and Dy metal atoms [88T, 93Y].

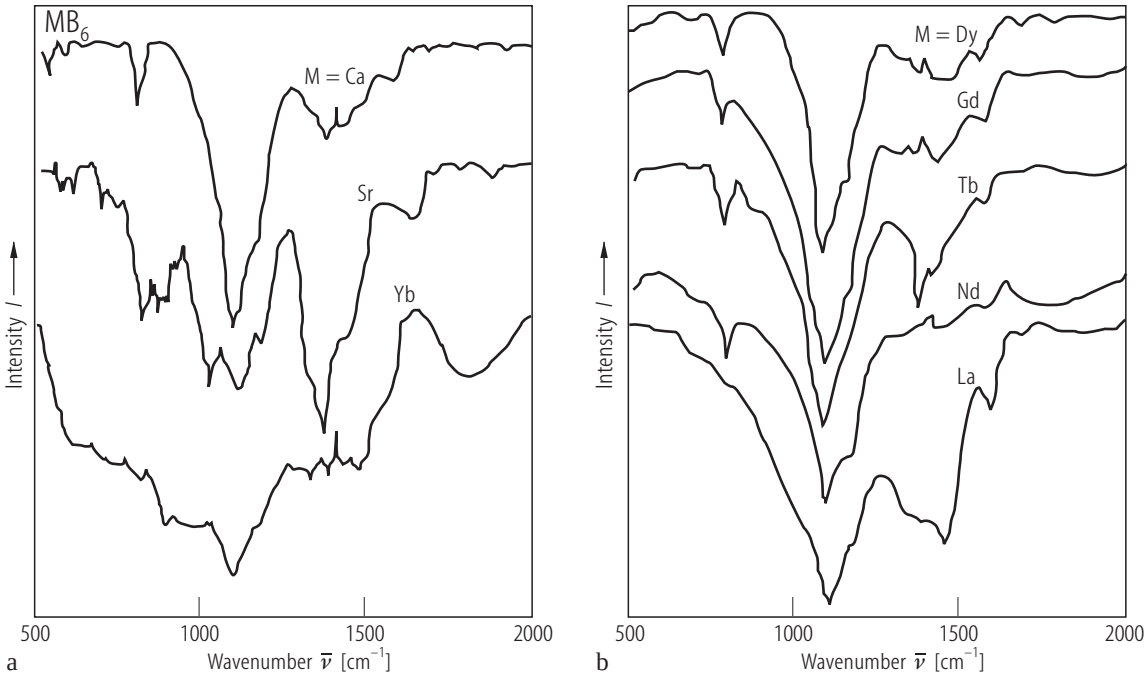

Fig. 14.

YbB_6. Reflectivity vs. wavenumber; for phonon frequencies (indicated by arrows) see lattice properties [99W].

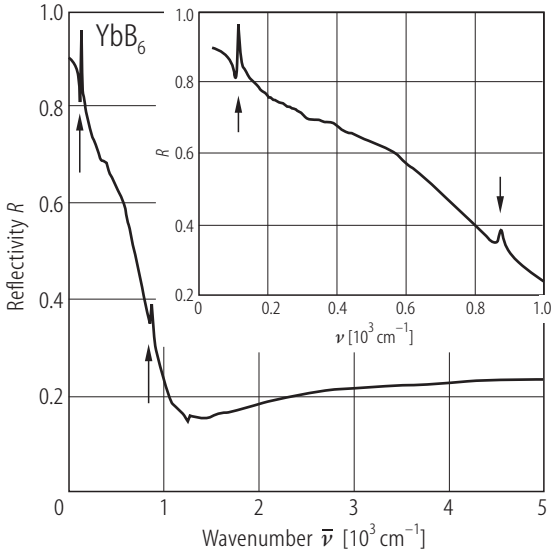

Fig. 15.

YbB_6. Specific heat C vs. T. Points experimental; solid line calculated from the total density of states; dashed line calculated from the acoustic modes only [85S].